Materials and Structures, 1992, **25**, 305–312

Measurement of the fracture energy using three-point bend tests: Part 2—Influence of bulk energy dissipation

J. PLANAS, M. ELICES, G. V. GUINEA

Departamento de Ciencia de Materiales, Escuela de Ingenieros de Caminos, Universidad Politécnica, Ciudad Universitaria, 28040 Madrid, Spain

Available measures of the fracture energy G_F obtained with the procedure proposed by RILEM TC-50 provide values that appear to change with sample size, calling into question whether G_F can be considered as a material parameter. In a previous paper, possible sources of energy dissipation from the testing equipment and lateral supports were considered. In this paper new possible sources of energy dissipation in the sample, apart from the fracture crack itself, are considered. Such dissipation will take place inside the bulk of the most stressed regions of the specimen and, if it is not taken into account, higher values of G_F will be recorded than that strictly due to surface fracture energy. When this contribution and the possible energy dissipation analysed in previous work are considered, they are not enough to account for the measured size effect. If G_F is to be considered a material parameter, the evaluation of the results from the RILEM method should be analysed more carefully. In any case, the dissipated energy reported here represents a non-negligible amount of G_F and should be taken into account when performing measurements.

1. INTRODUCTION

Available measures of the fracture energy G_F of cementitious materials obtained with the work of fracture method for notched beam tests [1] provide values depending on the sample size; in general, these values increase with sample size. A recent example was provided by a round-robin test. After comparing the results of a co-operative RILEM test – about 700 concrete beams of different sizes from fourteen laboratories – it was concluded that there was a size dependence of G_F [2].

Such results cast some doubts on the relevance of G_F. If G_F is to be considered a material property, it has to be size-independent. If G_F changes with specimen size, most available models to predict concrete fracture should be revised. Research aimed at discovering some sources of experimental errors that can explain the measured size dependence of G_F was therefore undertaken by the authors. In a previous paper [3] possible sources of energy dissipation in the testing equipment and in the rolling supports were analysed. Although some size-dependent energy dissipation was found in both cases, the measured values were not enough to account for the total observed size dependence of G_F.

The purpose of this paper is to explore new possible sources of energy dissipation in the sample, apart from the fracture crack surface itself. Such dissipation will take place inside the bulk of the most stressed regions of the specimen and, if not taken into account, higher values of G_F will be recorded than that strictly due to surface fracture energy. Moreover, if this extra dissipated energy increases with specimen size – a plausible guess – it might explain the observed size dependence of G_F.

2. BULK ENERGY DISSIPATION

To have a feeling for the more stressed regions during the beam test, a numerical computation based on the cohesive crack model [4] was performed. The fracture zone of the beam was modelled with a bilinear softening function, as shown in Fig. 1, and the bulk was considered linear elastic. The FEM computer code was ANSYS®. Concrete properties were $E = 27$ GPa, $\nu = 0.2$, $G_F = 100$ N m^{-1}, $f_t = 3.14$ MPa, $\sigma_c = 30$ MPa and critical crack opening $w_c = 114.6$ μm.

From the set of all situations along the path leading to the complete failure of the specimen, two situations were considered for special analysis. The first was that corresponding to the peak load. The second was that corresponding to an advanced state of crack growth, where the small uncracked ligament indicates that high compressive bending stresses might exist. Lines of constant maximum principal stress are depicted in Fig. 2a for the peak load situation. Fig. 2b shows the map of isolines for the minimum principal stress (maximum compressions). Similar results for the small uncracked ligament situation are shown in Fig 3a and b.

From these results it may be concluded that regions damaged by compressive loads are very much localized at the supports, and that the influence of a possible zone on the crack path damaged in compression prior to the tensile fracture is negligible. Moreover, a detailed analysis of the results shows that the high compressions are due to the point-load, not to the bending stresses. Regions that may be damaged due to tensile stresses have a kidney shape and develop beside the crack path. Another interesting result is that both regions – tensile and

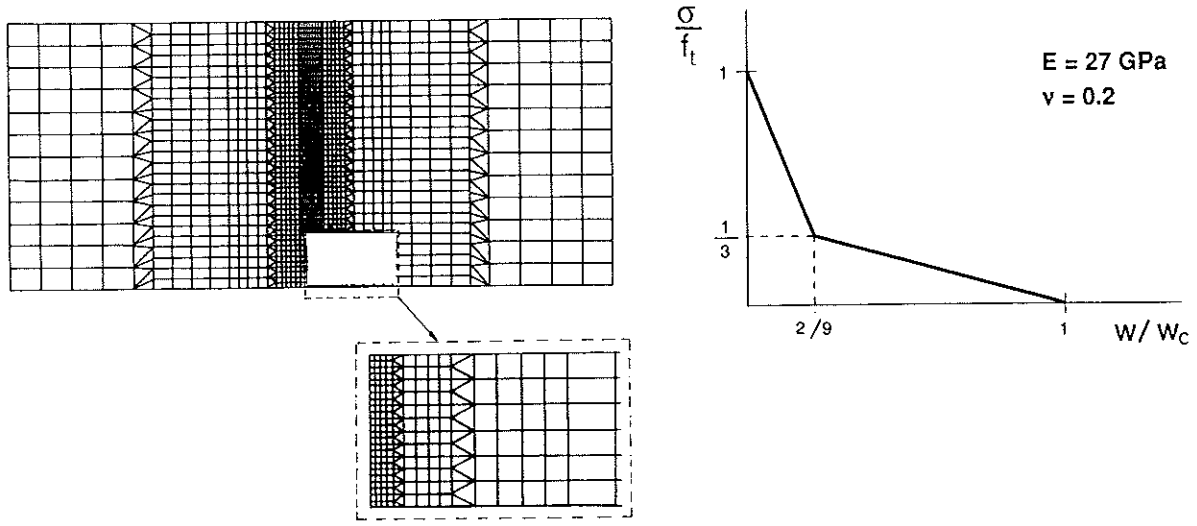

Fig. 1 Finite-element mesh and softening curve for the bulk-elastic analyses.

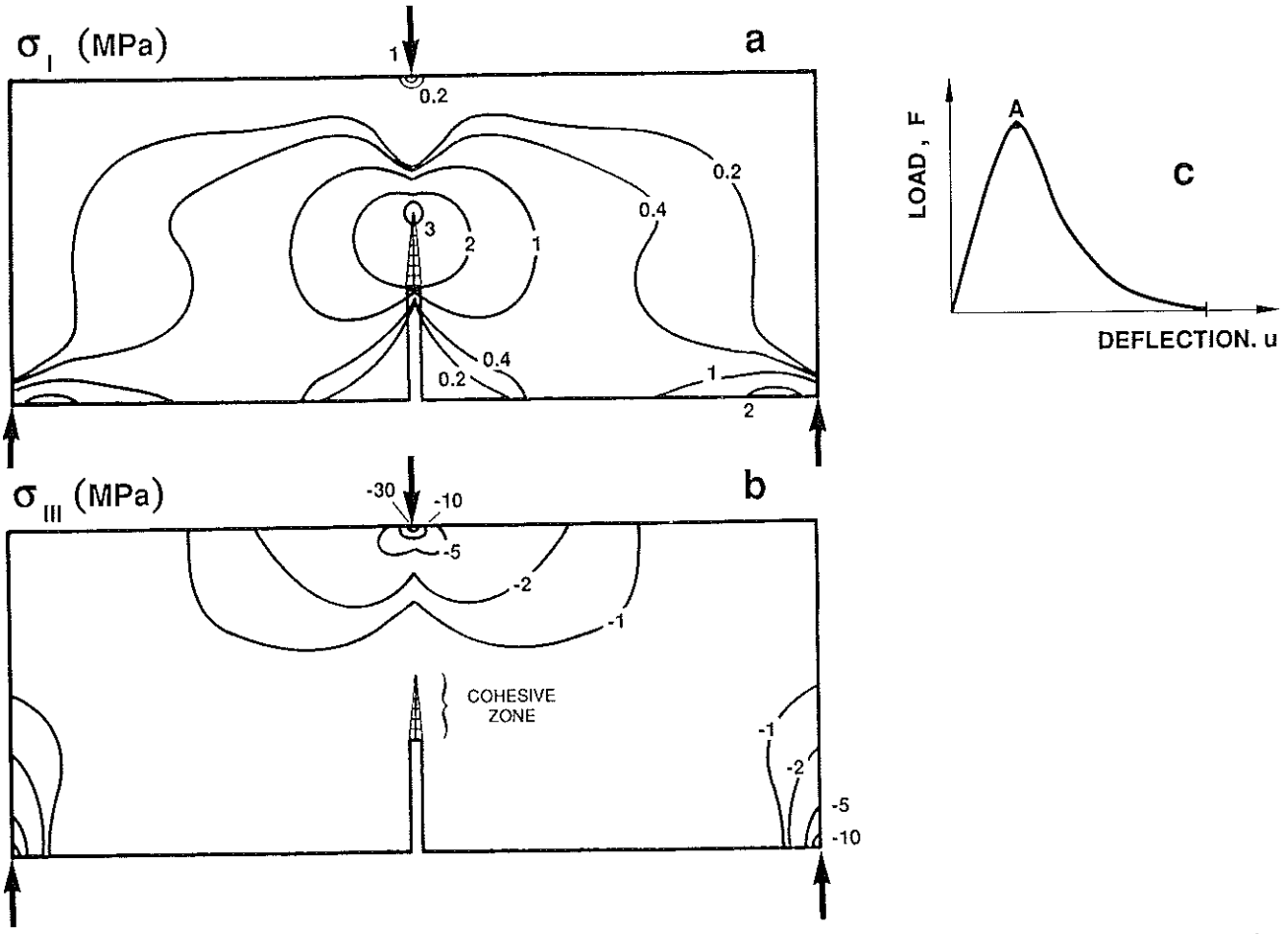

Fig. 2 Isolines for (a) maximum principal tensile stress and (b) minimum principal stress (compression negative) at the peak load situation (point A in (c)).

compressive – are clearly localized and separate from one another. Consequently they may be uncoupled and analysed separately, at least in a first approximation.

The theoretical analysis of energy dissipation around supports is a very involved problem, particularly for rolling lateral supports, where crushing and friction are coupled. A straightforward procedure is to measure this energy by a properly designed test. This solution was adopted successfully for lateral supports and the results were given in a previous paper [3]. A similar procedure

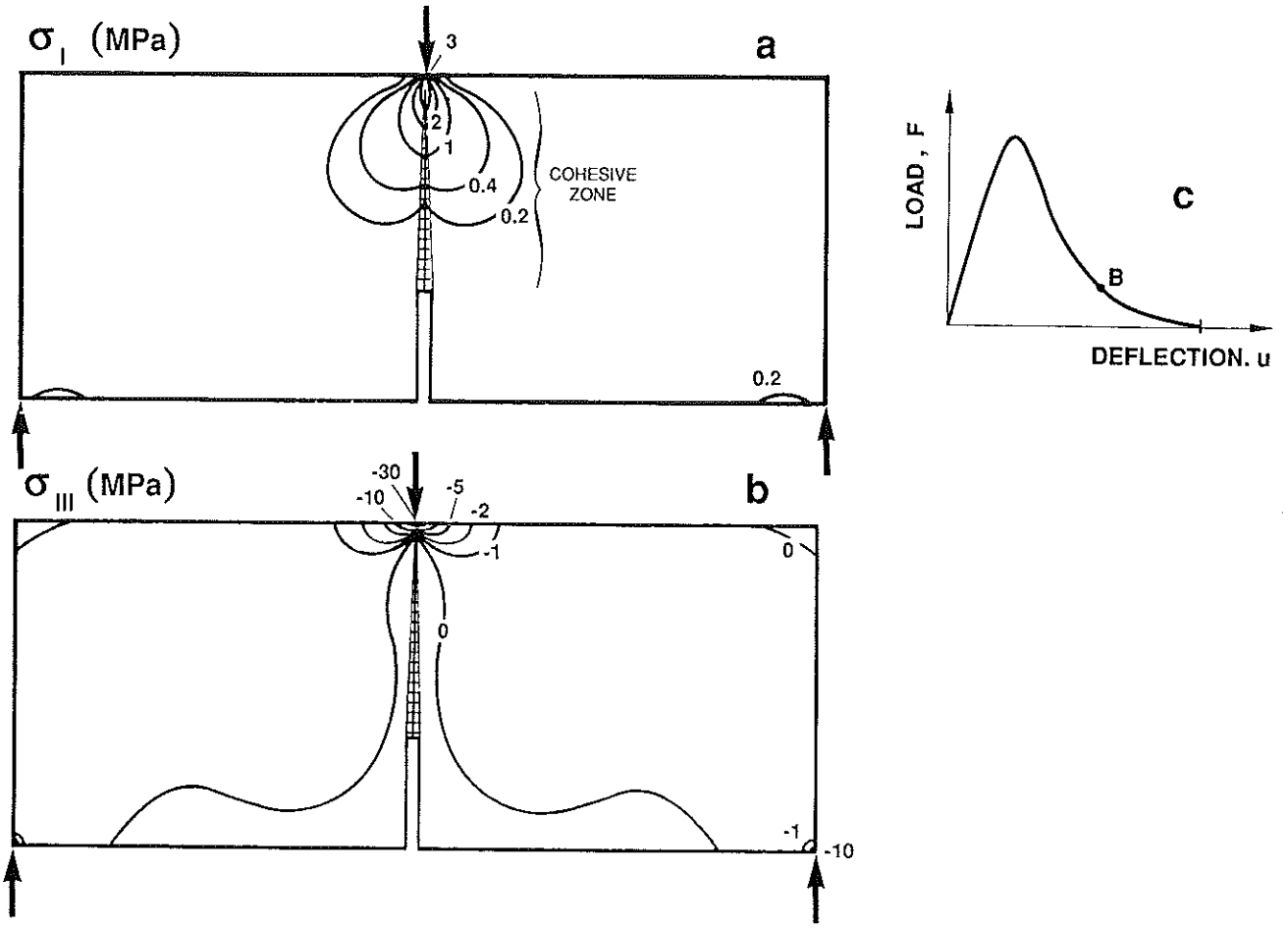

Fig. 3 Isolines for (a) maximum principal tensile stress and (b) minimum principal stress (compression negative), at advanced crack growth represented by point B on the load–displacement curve (c) where the load has dropped to 10% of the peak value.

is implemented here to measure the energy dissipation at the central support.

The evaluation of the energy dissipated due to tensile stresses in the bulk of the specimen – outside the crack plane – cannot be performed experimentally because there is no way to uncouple the energy dissipated in the bulk from that dissipated in the crack surface itself, mainly because both processes are intimately associated. Henceforth, a theoretical estimate will be given, based on an inelastic bulk model, together with simplified methods of numerical analysis (perturbation method). Finite sizes are analysed using standard FEM, and an upper bound for infinite size is obtained using an asymptotic analysis previously developed by the authors [5].

3. ENERGY DISSIPATION BELOW THE CENTRAL SUPPORT

As already mentioned, during the RILEM test some energy will be dissipated under the central support, following the process of loading and unloading. A numerical estimation of this energy is difficult because of the high triaxiality and the lack of a sound model for triaxial behaviour of concrete in compression. This is why a direct experimental method was selected.

The experiment is based on the hypothesis that the crushing zone below the support is essentially uncoupled from the crack growth process, in such a way that the process 'felt' by the crushing material is just a load rise followed by an unloading. We think then that the energy dissipated in this zone may be obtained by making a test where a single support is loaded up to the maximum load found in the fracture test and then unloaded, and where all other sources of energy dissipation (crack, friction, etc.) are ruled out. For further improvement, loading rates should be used similar to those found in actual fracture tests.

A sketch of the experimental set-up is shown in Fig. 4. Load was applied with the same device used for beam tests. The displacement, u, associated with the applied load was measured as sketched in Fig. 4. The sample dimensions were chosen so that maximum tensile stresses were always less than one-third of the concrete tensile strength, thus avoiding energy dissipation due to tensile damage.

The test consisted of loading and unloading the specimen and recording the load and its associated displacement. Six measurements were done for

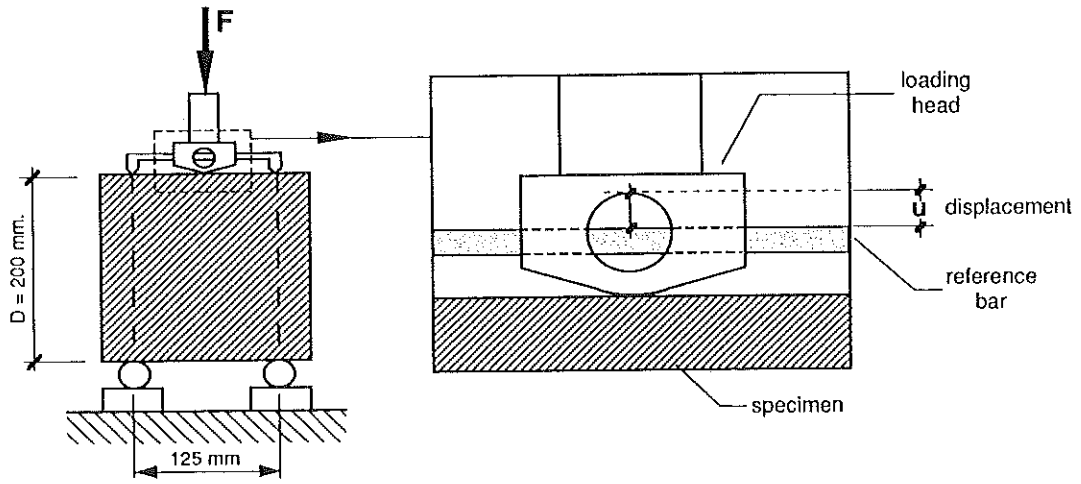

Fig. 4 Sketch of the experimental device for the determination of the dissipation at the central support. Specimen thickness 100 mm.

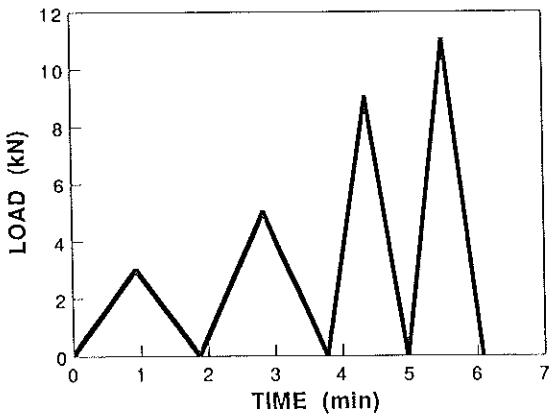

Fig. 5 Loading history for testing the central support. Each peak corresponds to a beam size.

every maximum load. The area enclosed along one cycle – virgin loading and unloading – gives the dissipated energy during this process. The cycle was different for each specimen size, depending on the maximum load reached during the RILEM test. The four cycles are shown in Fig. 5. The virgin loading curve was approximated by the envelope of the cyclic curve. The loading velocity was different for each test, depending on the maximum load, in order to reproduce the loading conditions of actual tested beams. Each maximum load is the average value of the peak load measured during the RILEM test for each specimen size.

Fig. 6a shows the measured energy dissipated at the central support as a function of the maximum load during the beam test. When this energy is divided by the broken area of the tested beam, to obtain a specific dissipated energy, a marked size effect appears, although for the largest size its contribution to G_F is less than 10%, as can be seen in Fig. 6b. In Part 3 of this work [6], recorded values of the size effect are about 50%. Again, this source of energy dissipation is not enough to account for the known size effect in G_F.

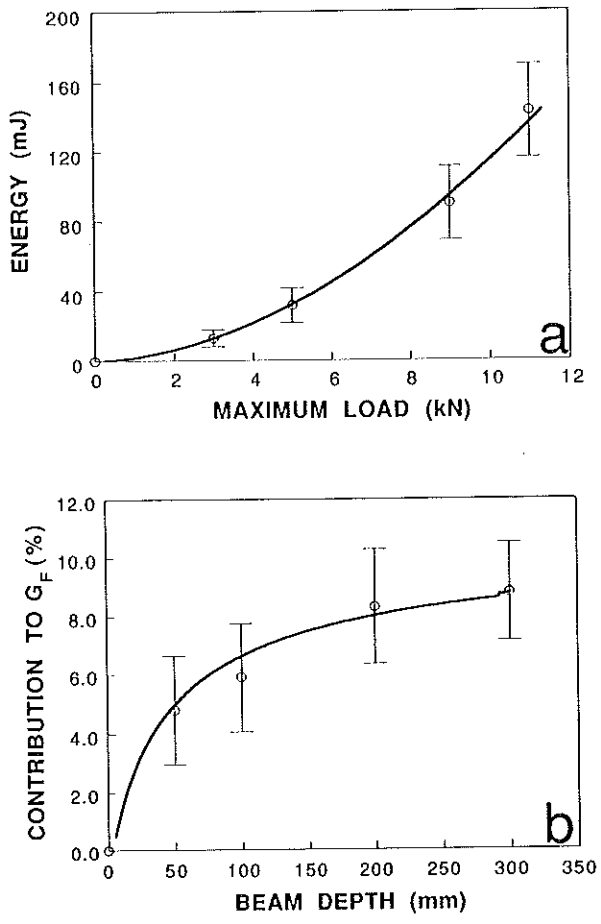

Fig. 6 Energy dissipated at the central support: (a) absolute value, (b) relative contribution to the measured fracture energy. Reference value, $G_F = 81\ N\ m^{-1}$).

4. BULK ENERGY DISSIPATION AT REGIONS OF HIGH TENSILE STRESSES

As shown in Figs 2 and 3, there are two regions attached to the crack path that support high tensile stresses. It might be expected that some energy would be dissipated

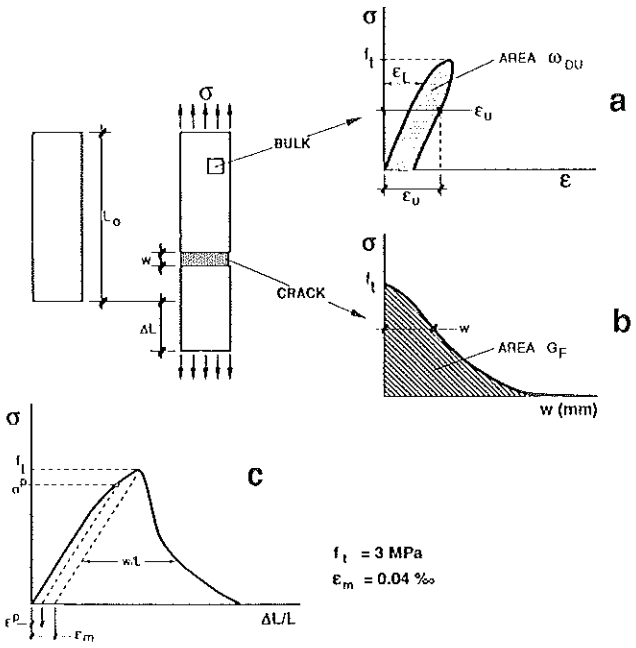

Fig. 7 Material model in tension: (a) bulk behaviour, (b) cohesive crack behaviour, (c) composite behaviour.

in these regions as the crack propagates. To evaluate this energy, an elasto-plastic numerical computation was performed. An upper bound was also derived based on an asymptotic analysis of a cohesive crack.

4.1 The model

The bulk behaviour of a dissipative concrete was modelled according to the concepts reported by Hillerborg [4]. A cohesive crack model displaying bulk dissipation is formulated by retaining the hypotheses regarding cohesive crack formation and evolution, and relaxing the hypothesis of linear elastic behaviour of the bulk.

For a simple uniaxial tensile test, performed under extension control, the stress–average strain sketched in Fig. 7 is found. The model is completely defined by a dissipative stress–*strain* relation in the loading branch previous to the peak (Fig. 7a) and by a stress–*crack opening* curve in the post-peak softening branch (Fig. 7b). The area within the loop in Fig. 7a is the dissipated energy per unit volume. In this model we consider a bulk stress–strain behaviour without stiffness degradation, so that the unloading proceeds along a straight line with the same slope as at initial loading (Fig. 7c).

In general, during crack propagation in the beam test, the bulk material close to the cohesive crack unloads – following a line parallel to the initial elastic branch, according to the previous hypothesis – leaving an irrecoverable strain, which in the uniaxial case is ε^p, variable with the previously reached level of stress σ^p (as shown in Fig. 7c). The relationship between ε^p and σ^p obtained from a uniaxial test will be the main input for this model, which, in order to be used in a non-homogeneous case, must be extended to triaxial situations. This extension was worked in detail in [7] using an internal variable formulation together with a thermodynamic approach, which allows the model to be extended to situations where stiffness degradation and irrecoverable strains are considered. In its present simpler form, it happens to coincide with an elasto-plastic model with a Rankine loading function and an associated flow rule.

The governing equations for this model may be written as

$$d\varepsilon = \boldsymbol{C}\, d\sigma + \boldsymbol{P}_1\, d\varepsilon^p \tag{1}$$

$$\varepsilon^p = f(\sigma^p) \quad \text{and} \quad \sigma^p = \mathrm{Sup}(\sigma_1) \tag{2}$$

Equation 1 is the well-known split of the incremental strain into elastic and irrecoverable parts. $\boldsymbol{C}$ is the elastic compliance fourth-order tensor and $\boldsymbol{P}_1$ defines the direction of plastic flow and is the projector tensor on the subspace associated with σ_1, the maximum principal stress. ε^p is the (uniaxial) equivalent plastic strain. The two Equations 2 are the hardening law and the integrated form of the Rankine load function $\sigma_1 \leq \sigma^p$. The hardening law is the only material function of the model. It is the relationship between the equivalent plastic strain and the instantaneous yield limit and is obtained from a uniaxial tensile stress–strain curve in the pre-peak branch, as sketched in Fig. 7. Finally, the *supreme* functional of the maximum principal stress is defined as

$$\mathrm{Sup}(\sigma_1) := \mathrm{Sup}[\sigma_1(\tau), t] = \max\{\sigma_1(\tau);\, \tau \in [0, t]\} \tag{3}$$

From Equations 1 and 2 one arrives at an equation relating the incremental strain tensor to the history of principal stresses:

$$d\varepsilon = \boldsymbol{C}\, d\sigma + \boldsymbol{P}_1 f'[\mathrm{Sup}(\sigma_1)]\, d[\mathrm{Sup}(\sigma_1)] \tag{4}$$

where $f'(x)$ indicates the first derivative of the function $f(x)$ with respect to its argument.

An interesting feature of this model is that the energy dissipated per unit volume ω^p, along any loading path, may be written in closed form as

$$\omega^p = \int_0^{\mathrm{Sup}(\sigma_1)} \sigma^p\, d\varepsilon^p = \int_0^{\mathrm{Sup}(\sigma_1)} \sigma^p f'(\sigma^p)\, d\sigma^p \tag{5}$$

The selected hardening law was

$$\varepsilon^p = f(\sigma^p) = 0 \qquad \text{for} \qquad \sigma^p/f_t \leq 0.5 \tag{6a}$$

$$\varepsilon^p = f(\sigma^p) = \varepsilon_m(2\sigma^p/f_t - 1)^2 \qquad \text{for} \qquad \sigma^p/f_t > 0.5 \tag{6b}$$

where f_t is the tensile strength and ε_m is the inelastic strain at the peak load, as shown in Fig. 7c. The softening function was taken to be the bilinear function previously used and sketched in Fig. 1.

4.2 Evaluation of the dissipated energy

The analysis of the development of a cohesive crack inside an elasto-plastic body is a complex task requiring powerful special-purpose numerical codes. However, it is possible to reveal the dominant effects by means of a first-order perturbation analysis set up by considering a

uniparametric family of elasto-plastic bodies where inelastic strain can be decreased uniformly to zero by writing the hardening function $f(\sigma^p)$ as $f(\sigma^p) = \lambda f^*(\sigma^p)$, which, according to Equation 4 leads to the incremental constitutive equation

$$d\varepsilon = \boldsymbol{C}\, d\sigma + \lambda \boldsymbol{P}_I f^{*\prime}[\mathrm{Sup}(\sigma_I)]\, d[\mathrm{Sup}(\sigma_I)] \qquad (7)$$

Obviously, when $\lambda \to 0$, the constitutive equation tends to the elastic form, so that at any loading step one can write the solution for the stress distribution as

$$\sigma = \sigma_0 + O(\lambda) \quad \text{and} \quad \mathrm{Sup}(\sigma_I) = \mathrm{Sup}(\sigma_{0I}) + O(\lambda) \qquad (8)$$

where $O(\lambda)$ and $O(\lambda)$ are, respectively, a tensor-valued function and a scalar-valued function vanishing for $\lambda \to 0$, and σ_0 and σ_{0I} are the bulk-elastic solutions for the stress tensor and the maximum principal stress. The dissipation density may then be written, according to Equation 5

$$\omega^D = \int_0^{\mathrm{Sup}(\sigma_{0I})} \sigma^p f'(\sigma^p)\, d\sigma^p + \lambda O(\lambda) \qquad (9)$$

The first-order approach for the dissipated energy is obtained by taking only the first term in Equation 9. Notice that for computing this value, one only needs the maximum stresses computed with the hypothesis of bulk linear elastic behaviour.

The dissipated energy was evaluated solving first the beam problem, as was done previously on other grounds, i.e. using finite elements with a cohesive crack embedded in a linear elastic medium, as sketched in Fig. 1. Then, the supreme of the major principal stress at each Gauss point was recorded along the process, and after complete fracture, the energy dissipated per unit volume was found using Equation 9. Volume integration (sum over elements) gave the total energy dissipation in the bulk. This result is depicted in Fig. 8a for the four sizes considered, as a function of the specimen size. The relative contribution of the bulk dissipation to the measured fracture energy is plotted in Fig. 8b.

4.3 An upper bound for the dissipated energy

Numerical results show two symmetrical regions, with respect to the crack plane, where energy can be dissipated as the crack propagates. An upper bound for this dissipation can be evaluated by considering an extreme situation: a very large specimen where the cohesive zone is fully developed and propagates in a self-similar way.

Moreover, when a first-order perturbation analysis is applicable, knowledge of the elastic solution suffices, as described in the previous paragraph. Fortunately, such a solution is known from work already done by the authors when analysing the asymptotic behaviour of cohesive cracks [5].

For very large specimens, and under steady-state propagation, the situation can be sketched as shown in Fig. 9, where this pattern moves self-similarly as the crack advances. Consequently, after a crack advancement of a, the dissipated energy per unit volume, $\omega^D(x_1, x_2)$, will

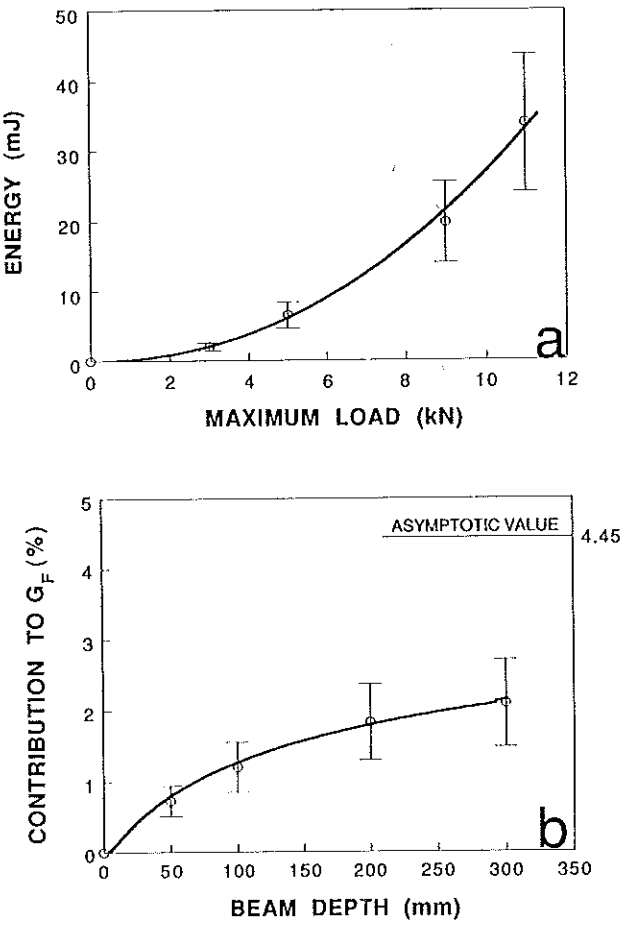

Fig. 8 Energy dissipated in the bulk tension zones: (a) absolute value, (b) relative contribution to the measured fracture energy, including the asymptotic value for infinite size.

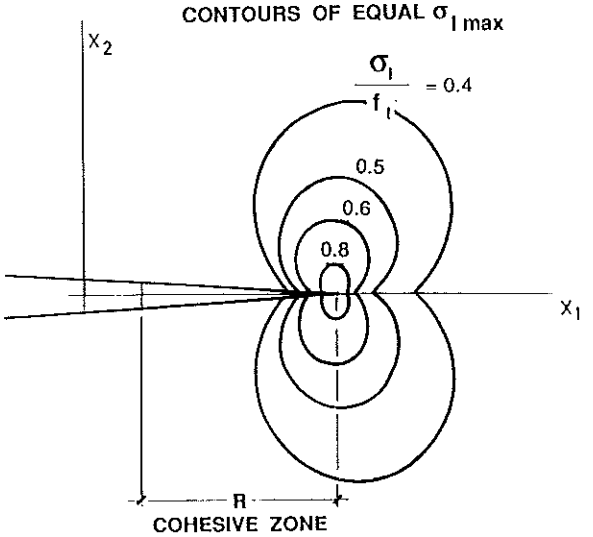

Fig. 9 Lines of equal maximum principal stress in steady-state growth of a cohesive crack in an infinite medium.

fulfil the conditions

$$\omega^D(x_1, x_2) = \omega^D(x_1 - a, x_2) \qquad (10a)$$

$$\frac{\partial \omega^D}{\partial a} = -\frac{\partial \omega^D}{\partial x_1} \qquad (10b)$$

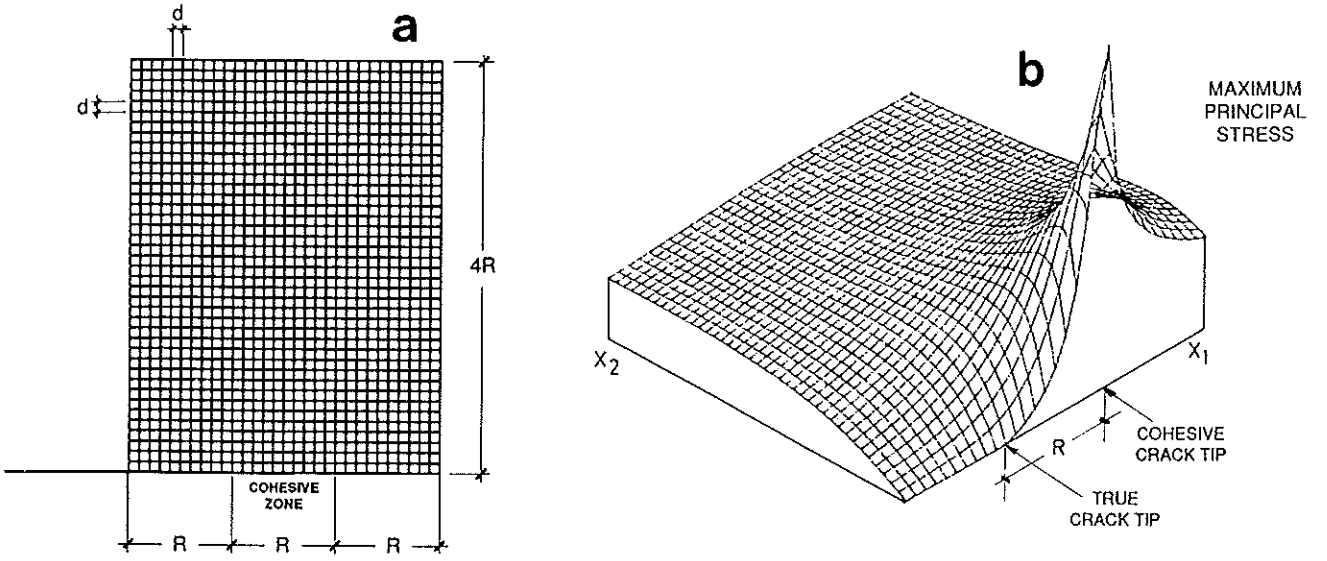

Fig. 10 (a) Grid used in the evaluation of the bulk dissipation for steady cohesive crack growth in an infinite medium. (b) Maximum principal stress distribution around the cohesive zone.

and the contribution of the bulk dissipation to the specific energy dissipation during crack growth is given by [7, 8]

$$\Delta G_F = \int_{-\infty}^{+\infty} \int_{-\infty}^{+\infty} \frac{\partial \omega^D}{\partial a} dx_1 \, dx_2 = \int_{-\infty}^{+\infty} \omega^D_{max}(x_2) \, dx_2 \tag{11}$$

where the second expression is obtained using Equation 10b, integrating with respect to x_1, and setting

$$\omega^D(\infty, x_2) = 0 \quad \text{and} \quad \omega^D(-\infty, x_2) = \omega^D_{max}(x_2).$$

These last equalities are easily found by taking into account that ω^D cannot decrease for a given material point, and that a point describes, with respect to the crack tip, a line x_2 = constant coming from $x_1 = \infty$ where the dissipated energy must be zero, and going to $x_1 = -\infty$, where the dissipated energy must be maximum. Of course, the maximum is attained much before reaching the minus infinite end of the line, exactly at the point where unloading starts, because in our model no energy dissipation takes place during unloading.

The maximum energy dissipation for a given ordinate, $\omega^D_{max}(x_2)$, when the perturbation approximation is used, is obtained from the elastic field of principal stresses, σ_{0I}, using Equation 9 with the only modification that $\mathrm{Sup}(\sigma_{0I})$ must be computed now as a spatial supreme rather than a temporal one:

$$\mathrm{Sup}(\sigma_{0I}) = \max\{\sigma_{0I}(x_1, x_2);\ x_1 \in (-\infty, +\infty)\} \tag{12}$$

When the hardening law shown in Equations 6a and 6b is used, ω^D_{max} becomes

$$\omega^D_{max} = \frac{f_t \varepsilon_m}{6}(16\beta^3 - 12\beta^2 + 1) \tag{13}$$

where $\beta = \mathrm{Sup}(\sigma_{0I})/f_t$.

To evaluate the dissipated energy, it suffices to know the values of $\mathrm{Sup}(\sigma_{0I})$ along x_2. These values can be extracted from the knowledge of the elastic solution. As already mentioned, this problem was solved by the authors for a general softening function [5]. Here, the maximum principal stresses were computed on a dense two-dimensional grid around the cohesive zone [7]. Fig. 10a shows the half grid (30 × 40 nodes) with $d = R/10$ (where R is the length of the steady cohesive zone), and Fig. 10b shows the distribution of the maximum principal stresses. By selecting the maximum stress along each line parallel to the crack line (x_2 constant), $\mathrm{Sup}(\sigma_{0I})$ was obtained and hence β. The dissipated energy was finally computed as

$$G_D = \sum_{\text{nodes}} \frac{f_t \varepsilon_m}{6}(16\beta^3 - 12\beta^2 + 1)d = 3.6 \text{ J m}^{-2} \tag{14}$$

This result is less than 5% of the specific fracture energy G_F, and does not account for the measured increase of G_F with specimen size, about 50% of G_F [6]. Other estimates of G_F, based on different realistic hardening functions, also give values much below $0.5G_F$ [7, 8]. The asymptotic result is drawn in Fig. 8b and shows that usual specimen sizes (up to 30 cm depth) are very far from the asymptotic limit.

5. CONCLUSIONS

The objective of this paper was to evaluate the energy dissipated inside the bulk of the most stressed regions of the notched beam, to ascertain whether this dissipated energy was size-dependent, and to check whether the computed values may account for the observed size effect.

1. Elastic analyses show that regions under high compressive stresses are localized at the supports. Results for lateral supports were already reported [3] and only the central support is considered here. Regions under

high tensile stresses develop along the crack path close to the tip and are also considered here. Highly compressed regions and highly tensioned ones are essentially uncoupled.

2. The specified dissipated energy at the central support is shown in Fig. 6b. It clearly exhibits a size effect, amounting to 10% of G_F for the largest size, but not enough to account for the measured values of size effect.

3. The specific dissipated energy inside the high tensile stress regions is shown in Fig. 8b. Again, a size effect appears, amounting to 2% of G_F for the largest size, not enough to explain the experimentally observed size effect. An asymptotic analysis was performed to obtain an upper bound, and values about 5% of G_F were found.

4. When all these contributions to energy dissipation are added together, including those reported earlier [3], they are not enough to account for the measured size effect – up to a 50% increase in G_F for a three-fold increase in size. If G_F is to be considered a material parameter, the evaluation of the results from the RILEM method should be analysed more carefully, as suggested in a subsequent paper [6].

In any case, the dissipated energy reported here represents a non-negligible amount of G_F and should be taken into account when performing measurements.

ACKNOWLEDGEMENTS

The authors gratefully acknowledge financial support for this research provided by the Comisión Interministerial de Ciencia y Tecnología (CICYT), Spain, under grant PB86-0494, and the Universidad Politécnica de Madrid, Spain, under grant A91 0020 02-31.

REFERENCES

1. RILEM TC-50 FMC (Draft Recommendation), 'Determination of the fracture energy of mortar and concrete by means of three-point bend tests on notched beams', *Mater. Struct.* **18**(106) (1985) 285–290.
2. Hillerborg, A., 'Results of three comparative test series for determining the fracture energy G_F of concrete', *ibid.* **18**(107) (1985) 407–413.
3. Guinea, G. V., Planas, J. and Elices, M., 'Measurement of the fracture energy using three-point bend tests: 1 – Influence of experimental procedures', *ibid.* **25**(148) (1992) 212–218.
4. Hillerborg, A., 'The theoretical basis of a method to determine the fracture energy G_F of concrete', *ibid.* **18**(106) (1985) 291–296.
5. Planas, J. and Elices, M., 'Un nuevo método de análisis del comportamiento asintótico de una fisura cohesiva en modo I', *Anales de Mecánica de la Fractura* **3** (1986) 219–227.
6. Elices, M., Guinea, G. V. and Planas, J., 'Measurement of the fracture energy using three-point bend tests: 3 – Influence of the P–δ tail', *Mater. Struct.* in press.
7. Guinea, G. V., 'Medida de la Energía de Fractura del Hormigón', PhD thesis, E.T.S. Ingenieros de Caminos, Universidad Politécnica de Madrid (1990).
8. Guinea, G. V., Planas, J. and Elices, M., 'Influencia de la disipación volúmica en la energía específica de fractura del hormigón', *Anales de Mecánica de la Fractura* **7** (1990) 211–217.

RESUME

Mesure de l'énergie de rupture par les essais de flexion trois points: 2 – Influence de la dissipation de l'énergie dans la masse

Les mesures de l'énergie de rupture G_F obtenues selon la méthode préconisée par la Commission Technique 50 de la RILEM, dont on dispose, changent avec la taille de l'éprouvette, ce qui met en question la possibilité de considérer G_F comme un paramètre du matériau. On a considéré, dans un article précédent, les sources possibles de dissipation de l'énergie due à l'équipement d'essai et aux supports latéraux.

On examine dans cet article-ci de nouvelles sources éventuelles de dissipation de l'énergie dans l'éprouvette, excepté celle de rupture proprement dite. Cette dissipation se produira dans la masse, dans les régions les plus contraintes de l'éprouvette et, si on n'en tient pas compte, on enregistrera des valeurs de G_F plus élevées que celles strictement inhérentes à l'énergie de rupture superficielle. Si on considère cet apport et la dissipation d'énergie éventuelle analysée dans le travail précédent, ils ne suffisent pas à expliquer l'effet d'échelle mesuré. Si on doit considérer G_F comme un paramètre du matériau, il conviendrait d'analyser avec plus de soin l'évaluation des résultats obtenus avec la méthode RILEM. De toute façon, l'énergie dissipée, dont on fait mention ici, représente une part non négligeable de G_F et devrait être prise en compte dans les mesures.